Limit-state function sensitivity under epistemic uncertainty: a convex model approach

Haodong Zhao[1], Changcong Zhou[2], Qi Chang[3], Haotian Shi[4], Marcos A. Valdebenito[5], Matthias G.R. Faes[6]

Abstract: This work proposes a limit-state sensitivity index to identify the input variables of a structure or system which possess a significant impact on its state for the case where the input variables are subject to epistemic uncertainty. By introducing the concept of a non-probabilistic limit-state measure, the proposed sensitivity index can represent the individual or joint influence of the input parameters. The proposed sensitivity index is applicable in conjunction with different convex set models, such as the hyper-rectangular or hyper-ellipsoidal models, as well as hybrid models. The basic properties of the sensitivity index are discussed in detail and its numerical estimation form is carried out. Two test examples are presented to prove efficiency, and a comparison with two existing sensitivity indices is also performed. Finally, the proposed sensitivity index is applied to the sensitivity analysis of a composite radome structure to quantify the influence of interval variables on the maximum displacement and total strain energy.

Keywords: Epistemic uncertainty; Interval; Non-probabilistic; Sensitivity analysis; Kriging

---

[1] Ph.D. Candidate, Department of Engineering Mechanics, Northwestern Polytechnical University, Youyi West Road 127, 710072 Xi’an, China. Email: hdzhao@mail.nwpu.edu.cn

[2] Professor, Department of Engineering Mechanics, Northwestern Polytechnical University, Youyi West Road 127, 710072 Xi’an, China (corresponding author). Email: changcongzhou@nwpu.edu.cn

[3] Ph.D. Candidate, Department of Engineering Mechanics, Northwestern Polytechnical University, Youyi West Road 127, 710072 Xi’an, China. Email: qichang@mail.nwpu.edu.cn

[4] Ph.D. Candidate, Department of Engineering Mechanics, Northwestern Polytechnical University, Youyi West Road 127, 710072 Xi’an, China. Email: haotian.shi@mail.nwpu.edu.cn

[5] Chief Engineer, Chair for Reliability Engineering, TU Dortmund University, Leonhard-Euler-Strasse 5, 44227 Dortmund, Germany. Email: marcos.valdebenito@tu-dortmund.de

[6] Professor, Chair for Reliability Engineering, TU Dortmund University, Leonhard-Euler-Strasse 5, 44227 Dortmund, Germany. Email: matthias.faes@tu-dortmund.de

Introduction

Uncertainties are often encountered in practical engineering structures and systems. In their turn, these uncertainties cause uncertainty in the corresponding performance of the structure or system. For instance, due to machining of components, uncertainties are introduced due to the limitations of the processing level, or the material preparation process. After the structural components are assembled, uncertainties such as material properties and working environment interact with each other, which can result in the occurrence of unforeseen structural failure or other serious accidents. Therefore, researchers in different fields have focused on improving the safety and robustness of structures by using uncertainty quantification (UQ) methods (Simoen et al. 2015)(Song et al. 2015).

Uncertainty can be divided into aleatory uncertainty and epistemic uncertainty based on its sources and attributes (Helton 1997). Aleatory uncertainty refers to the inherent randomness of parameters that cannot be reduced or eliminated, for example, the inherent random attributes of the dimension parameters of structural components in the same batch. The aleatory uncertainty is generally characterized by a probabilistic model. Epistemic uncertainty is caused by factors such as incomplete or inaccurate information, which can be reduced or eliminated when more information becomes available. A typical example of the latter refers to the uncertainties in the estimation of distribution parameters with limited sample size. Epistemic uncertainty is generally characterized by non-probabilistic models (such as convex sets and fuzzy models) (Naskar et al. 2019)(Hanss 2002).

The existence of uncertainties often may lead to deviations of the structural output response from the anticipated behaviour, and may cause reliability-related issues in structural systems. The term “reliability” usually refers to a probabilistic concept for quantifying the probability of the structure achieving the predetermined performance. Reliability analysis methods based on the rigorous axioms of probability theory have been developed in recent decades, and have been successfully applied to numerous engineering problems (Pradlwarter et al. 2005)(Goller et al. 2013). However, probabilistic models often rely on considerable amounts of sample data to obtain accurate probability distribution information of variables. When these sample data are not available, one risks that the modelled aleatory uncertainty is “buried” underneath the epistemic uncertainty stemming from the estimation of the probabilistic model under insufficient data. At the same time, due to high experimental costs, data collection is often difficult, and accurate variable distribution information cannot be obtained directly. On top, the application of probabilistic models for the case where only epistemic uncertainty is considered, may be questionable (Faes and Moens 2020)(Faes et al. 2021). These arguments illustrate the need for developing also dedicated methods to deal with specifically epistemic uncertainty, such as, e.g., interval and convex set models.

The interval model has been used to describe the uncertainty-but-bounded epistemic parameters encountered in mechanical analysis processes (Ben-Haim 1993)(Elishakoff et al. 1994). Currently, the hyper-rectangular model and the hyper-ellipsoid model are the commonly used non-probabilistic convex set models (Jiang et al. 2018)(Guo and Lu 2015). Generally, the hyper-rectangular model describes variables that are bounded, while the hyper-ellipsoid model describes variables that are bounded and that exhibit a dependence structure. Furthermore, Faes and Moens (Faes and Moens 2019) developed an interval-valued equivalent method to the well-known Copula pair constructions for handling the dependence case in the hyper-rectangular model. In practical engineering problems, the two aforementioned models often exist simultaneously, where some variables have the same or similar sources, resulting in dependence, while other variables have different sources and are not dependent. In addition, a multidimensional parallelepiped model proposed by Jiang et al. (Jiang et al. 2014) also provided a promising method for UQ. However, the mathematical formulation of the multidimensional parallelepiped model may be challenging for practical applications (Ni et al. 2016). Based on the concept of hyper-rectangular and hyper-ellipsoid models, Guo and Lu (Guo and Lu 2015) analogized the probabilistic reliability index and proposed a "non-probabilistic reliability index", which provided a quantitative index to measure the ability of a structure to exhibit a certain performance under epistemic uncertainty. However, this index does not convey information about reliability, but only about the state of a system. Thus, it is impossible to attribute a "reliability" to this index and hence, in this work, we use the term "non-probabilistic limit-state measure" to evaluate the state of a structure to complete predetermined performances (Ben-Haim 1994).

Analysing and quantifying the ability of a system to exhibit an acceptable performance is a central task of uncertainty quantification, irrespective of the use of probabilistic or non-probabilistic method. In addition, an equally important task is conducting sensitivity analysis. In essence, sensitivity analysis aims to measure the impact of an input variable (with its associated uncertainty) on the output response of a model (Wei et al. 2015)(Zhou et al. 2021b). Common sensitivity analysis methods mainly include local sensitivity analysis (LSA) and global sensitivity analysis (GSA) (Kala 2020). LSA is usually cast in terms of the partial derivatives of the output response to the parameters of input variables, which reflects the influence of local changes in the parameters on the output response. GSA on the other hand measures the contributions of input variables to the output response by considering the whole uncertainty range. Currently, variance-based sensitivity indices, which include the first-order sensitivity index and total effect sensitivity index, are widely studied and used (Saltelli 2002)(Papaioannou and Straub 2021). In addition to using variance as the definition of the sensitivity index, Borgonovo's sensitivity index defined by moment independence has also been studied (Zhou et al. 2021b)(Borgonovo 2007). To the best of our knowledge, most of the existing sensitivity indices aim at probabilistic models.

Equivalently, sensitivity analysis for interval and convex set models has attracted the attention of researchers in recent years to assess the sensitivity of the output uncertainty on the epistemic uncertainty on the input of the model (Faes and Moens 2020). Sensitivity indices for epistemic uncertainty are especially useful to answer the question "which input parameters are the most useful to collect extra data on, as to reduce our epistemic uncertainty". Moens and Vandepitte (Moens and Vandepitte 2007) first introduced the sensitivity analysis to interval analysis and proposed a novel sensitivity index to quantify the relationship between the change in absolute interval radius on the input and the output side of the problem. Chang et al. (Chang et al. 2022) proposed a new sensitivity index to quantify the individual or joint influence of the interval variables on the output. However, above two sensitivity indices do not directly consider the influence of variables on non-probabilistic performance. Li et al. (Li et al. 2013) proposed two sensitivity indices based on the non-probabilistic state measure, i.e., the shape effect index and position effect index. These two sensitivity indices provide a feasible way to quantify the influence of variables on structural performance under epistemic uncertainty. However, the importance ranking of influence on structural performance often requires a combination of these two sensitivity indices. When the ranking results of the two sensitivity indices are different, ambiguity will occur. In summary, currently available sensitivity indices can only provide limited information on the impact of input uncertainty on the system's response under non-probabilistic models. On top, they do not provide any information about the limit-state behaviour of the structure subjected to this information. This, however, is of major interest when an analyst wants to ensure the safety of their structure under the governing epistemic uncertainty.

Inspired by previous works, we propose a new sensitivity index applicable to the convex set model that can additionally provide guidance for improving the performance of a system. First, this sensitivity index is defined with respect to the so-called non-probabilistic performance measure. As such, the obtained sensitivity index results directly provide guidance for improving the non-probabilistic performance. Second, to improve the generality of the proposed sensitivity index, this sensitivity index is extended such that it is applicable with both the hyper-ellipsoid model and a hybrid model (in which interval and hyper-ellipsoid models co-exist simultaneously). In conclusion, the proposed sensitivity index in this work focuses on the sensitivity analysis of epistemic uncertainty, which is a common case in engineering.

The remainder of this work is organized as follows. First, the basic theory of non-probabilistic convex set models and the meaning of non-probabilistic limit-state measure are reviewed. Thereafter, a new sensitivity index based on non-probabilistic limit-state measure is defined, and a method for calculating the proposed sensitivity index is presented. To illustrate the effectiveness of the proposed sensitivity index, two numerical examples and an engineering problem involving a honeycomb sandwich radome are investigated. Finally, the conclusions are drawn.

Brief review of non-probabilistic convex set models

In this section, the basic theory of non-probabilistic convex set models is reviewed, and the non-probabilistic limit-state measure is explained. It should be pointed out that while the original formulations of this metric are developed by Guo and Lu (Guo and Lu 2015), in this work, we do however propose a re-classification of this metric to make it also valid under the axioms of interval theory.

Hyper-rectangle model and hyper-ellipsoid model

In the non-probabilistic convex set models, the hyper-rectangle model and the hyper-ellipsoid model are the commonly used approaches for characterizing variables with uncertain-but-bounded uncertainty (Faes and Moens 2020)(Guo and Lu 2015). The major difference between these two models is the existence of dependence between variables. The hyper-rectangle model describes variables that are bounded, while the hyper-ellipsoid model describes variables that are bounded, and which are also dependent. In the hyper-rectangle model, the uncertainty associated with interval $\boldsymbol{X}^{\boldsymbol{I}} = [X_1^I, X_2^I, ..., X_n^I]$ is represented by

$$\boldsymbol{X}^{\boldsymbol{I}} = X_1^I \times X_2^I \times ... \times X_n^I, \text{ with } X_i^I = \left\{ X_i \,\middle|\, \left| X_i - X_i^c \right| \le X_i^r \right\} \tag{1}$$

where X_i^c $(i = 1,...,n)$ denotes the centre value, collecting the centres of the interval variables X_i which is calculated as $X_i^c = \dfrac{X_i^U + X_i^L}{2}$; X_i^r denotes the radius vector, collecting the individual interval radius $X_i^r = \dfrac{X_i^U - X_i^L}{2}$; X_i^U and X_i^L denote the upper and lower bounds of X_i^I; and $|.|$ denotes absolute operator. It should be noted that $\boldsymbol{X}^{\boldsymbol{I}}$ effectively bounds a hyper-rectangular space in $\mathbf{R}^n$ due to the Cartesian product in Eq.(1). This implies that all X_i^I, X_j^I are orthogonal to each other, and hence, cannot encode any dependence. The work of Faes and Moens effectively bypasses this independence by means of the so-called Admissible Set Decomposition (Faes and Moens 2019).

If dependence exists among the interval variables $\boldsymbol{X} = [X_1, X_2, ..., X_n]$, then that dependence can be alternatively also captured by the hyper-ellipsoid model defined as (Ben-Haim and Elishakoff 1990):

$$\boldsymbol{X}^{\boldsymbol{I}} = X_1^I \times X_2^I \times ... \times X_n^I, \text{ with } \boldsymbol{X}^{\boldsymbol{I}} = \left\{ \boldsymbol{X}^{\boldsymbol{I}} \,\middle|\, (\boldsymbol{X} - \boldsymbol{X}^c)^T \boldsymbol{W} (\boldsymbol{X} - \boldsymbol{X}^c) \le \theta^2 \right\} \tag{2}$$

where $\theta \in \mathbf{R}^+$ denotes the radius of the ellipsoid and defines the magnitude of the uncertainty, and $\boldsymbol{W} \in \mathbf{R}^{n \times n}$ is a symmetric positive-definite matrix that contains the dependence information of variables. When only two variables are dependent and $\boldsymbol{W}$ is a diagonal matrix, Eq.(2) can be rewritten as a two-dimensional ellipse equation

$$\frac{(X_i - X_i^c)^2}{(X_i^r)^2} + \frac{(X_j - X_j^c)^2}{(X_j^r)^2} \le 1, \tag{3}$$

The two-dimensional convex set models, including the hyper-rectangle model and hyper-ellipsoid model, are depicted in Figure 1. The blue rectangle represents the domain of the hyper-rectangle model, and the orange ellipse represents the domain of the hyper-ellipsoid model in Figure 1 (a). Due to the existence of dependence, the hyper-ellipsoid model contains a smaller domain than the hyper-rectangle model under the same inequality value, as shown in Figure 1 (b) and (c). This makes sense from an epistemic uncertainty point of view. Indeed, when adding dependence to the uncertain quantities (as is the case in the ellipsoid model), one adds information to the analysis that effectively reduces the epistemic uncertainty in the system.

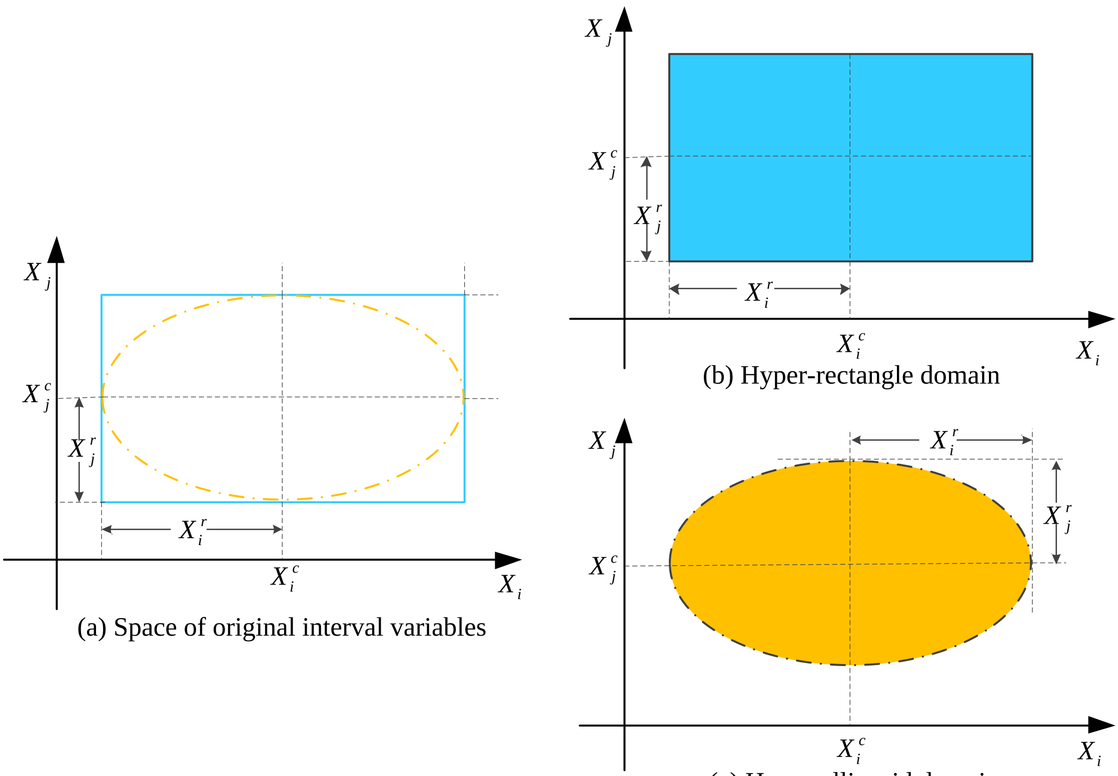

(a) Space of original interval variables

(b) Hyper-rectangle domain

(c) Hyper-ellipsoid domain

Figure 1 Schematic illustration of the two-dimensional convex set models

For the sake of simplicity, the normalized form of the interval variables is commonly used and represented as

$$\delta_i = (X_i - X_i^c) / X_i^r \,, \tag{4}$$

and

$$\delta_j = \boldsymbol{Q}_j (\boldsymbol{X} - \boldsymbol{X}^c) / \theta \,, \tag{5}$$

where $\boldsymbol{Q}_j$ denotes the *j*-th row of the matrix $\boldsymbol{Q}$ and where $\boldsymbol{Q} \in \mathbf{R}^{n \times n}$ is the upper triangular matrix satisfying the Choleski decomposition $\boldsymbol{W} = \boldsymbol{Q}^{\mathrm{T}} \boldsymbol{Q}$. By applying the above transforms, the original interval variables turn into standardized interval variables $\delta_i \in \delta_i^I = [-1,1]$, $\delta_j \in \delta_j^I = [-1,1]$ (Wang et al. 2018). The superscript '*I*' denotes the interval.

As shown in Figure 2, after applying standardization, the rectangular and elliptical domains are transformed into the domains illustrated by the blue square and dashed yellow circle, where the circle is circumscribed to the square.

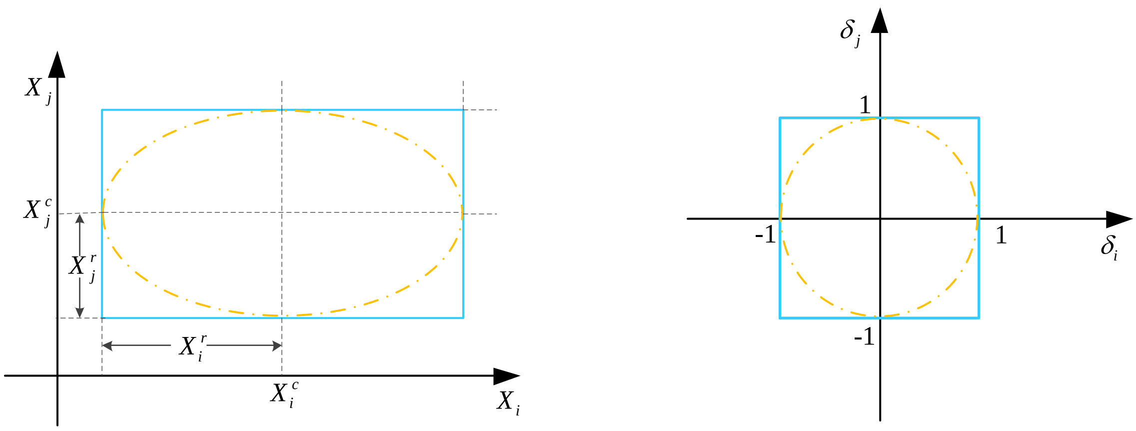

(a) Space of original interval variables (b) Space of standard interval variables

Figure 2 Space transform of interval variables

A non-probabilistic limit-state measure

The performance function is a classical concept in probabilistic reliability analysis, which is helpful for monitoring one or more responses of interest of an engineering system (Bichon et al. 2008). In principle, this performance function is also useful within the context of non-probabilistic uncertainty analysis and is defined as:

$$M = G(\boldsymbol{X}) = G(X_1, ..., X_n) \,, \tag{6}$$

where $G(\boldsymbol{X})$ is the performance function, and $\boldsymbol{X} \in \boldsymbol{X}^I$ denotes the vector of interval variables. $G(\boldsymbol{X}) = 0$

denotes the limit-state function (LSF), which divides the input space into the safe domain $G(\boldsymbol{X})>0$ and the failure domain $G(\boldsymbol{X})\le 0$. After the normalization mentioned in last section, the performance function in the standardized variable space is represented by $g(\boldsymbol{\delta})$. The failure domain is then denoted as $g(\boldsymbol{\delta})\le 0$ (as shown in Figure 3). Because the standardization of the variables has no actual effect on the value of the performance function, the symbol M is still used to represent the performance function in the standardized variable space, i.e., $M=g(\boldsymbol{\delta})$. Obviously, the value of $g(\boldsymbol{\delta})$ is an interval quantity because it is a continuous function of interval variables δ, so the interval of performance function M^I is defined as follows:

$$M^I=[M^L,M^U]=[\min_{\delta\in\delta^I} g(\boldsymbol{\delta}),\max_{\delta\in\delta^I} g(\boldsymbol{\delta})] \quad . \tag{7}$$

Analogous to the reliability index in the probability model, Guo and Lu (Guo and Lu 2015) defined the "non-probabilistic reliability index" η as follows:

$$\eta=\frac{M^c}{M^r}, \tag{8}$$

where $M^c=\dfrac{M^U+M^L}{2}$ denotes the centre value of M^I, and $M^r=\dfrac{M^U-M^L}{2}$ denotes the radius of M^I.

The minimum value of η is set as 0 because it is meaningless when $\eta<0$ in practice. It should be noted that although Guo and Lu named the quantity η as a "non-probabilistic reliability index", the name "non-probabilistic limit-state measure" may reflect its properties better. To substantiate the latter assertion, consider the schematic representation in Figure 3. When a linear performance function is used to derive non-probabilistic limit-state measure η considering the hyper-rectangle model, it can be seen that the value of this index is the same as the shortest distance measured by the infinite norm from the coordinate origin to the LSF in the standard variable space (Guo and Lu 2015). Thus, the definition of non-probabilistic limit-state measure for the hyper-rectangle model can be rewritten as

$$\begin{cases}\eta^{HR}=\min(\|\boldsymbol{\delta}\|_\infty)\\ s.t.\ \ M=G(\boldsymbol{\delta})=0\end{cases} \tag{9}$$

where $\|.\|_\infty$ denotes the infinite norm operator, and HR is the abbreviation of hyper-rectangle. When considering the hyper-ellipsoid model, the 2-norm is used to extend the definition of the non-probabilistic limit-state measure due to elliptic equation constraints on the dependence of variables (Guo and Lu 2015),

$$\begin{cases} \eta^{HE} = \min(\|\boldsymbol{\delta}\|_2) \\ s.t.\ \ M = G(\boldsymbol{\delta}) = 0 \end{cases} \tag{10}$$

where $\|\cdot\|_2$ denotes the 2-norm operator, and HE is the abbreviation of hyper-ellipsoid. Eq.(9) and Eq.(10) reflect the geometric interpretation of η^{HR} and η^{HE}, i.e., the shortest distance from the origin to LSF measured by infinite norm or 2-norm in the standard variable space. The above indices for the two types of convex set models are represented by solid blue lines and dotted yellow lines in Figure 3.

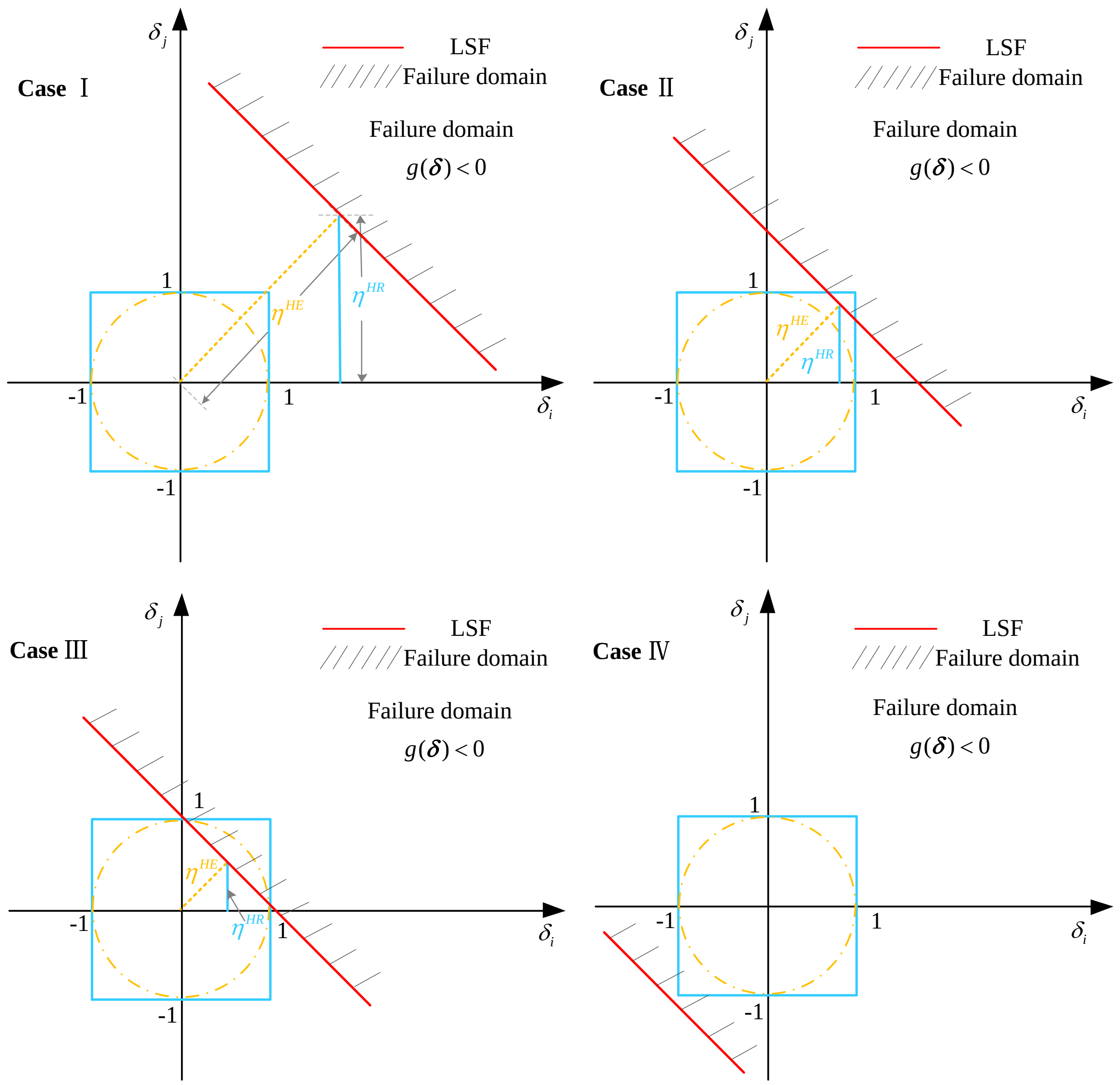

Figure 3 Schematic illustration of the non-probabilistic limit-state measure η.

Four cases of relative positions of LSF (denoted by the red line in Figure 3) and standardized two-dimensional variable space are used to further illustrate the relationship between the non-probabilistic limit-state measure η

and the state of a system, and the different cases are discussed as follows.

Case I: The normalized hyper-rectangle domain and hyper-ellipsoid domain do not intersect with the failure domain, which indicates that the structure is safe and the non-probabilistic limit-state measures are such that $\eta^{HE} > \eta^{HR} > 1$. Practically speaking, this means that the structure is safe, according to the modelled epistemic uncertainty.

Case II: The normalized hyper-rectangle domain intersects with the failure domain, and the normalized hyper-ellipsoid domain does not intersect with the failure domain. Thus, the structure is safe when uncertainty is measured by the hyper-ellipsoid model but may fail when considering the hyper-rectangle model, and $\eta^{HE} > 1 > \eta^{HR}$. Practically speaking, the structure might be safe when the dependence is modelled accurately, but unsafe when the dependence between the different X_i is ignored. The prudent engineering way to deal with this is to assess the trustworthiness of the modelled dependence.

Case III: The normalized hyper-rectangle and the hyper-ellipsoid domain intersect with the failure domain, which indicates that the structure is in a failure or safe state and $\eta^{HR} < \eta^{HE} < 1$. As such, failure might occur because of certain realisations of the epistemic uncertainty. It is however impossible to assess the likelihood of such failure. The prudent way forward would be to try and reduce the epistemic uncertainty to be able to make a more precise estimate.

Case IV: The two domains associated with the hyper-rectangle and hyper-ellipsoid models are fully located in the failure domain, which indicates that the structure is in a failure state for every possible realisation of the epistemic uncertainty.

From the above discussions, the value of η reflects the state of the structure. Indeed, whenever $\eta > 1$, the system is in a safe state. Conversely, whenever $\eta = 0$, the system has failed. Since, by definition, no information on the relative likelihood of certain parameter values within the bounds of the interval/convex set are known, whenever $0 < \eta < 1$, it is unknown whether the system is in a safe or failure state. From the last assertion, it becomes clear that the index η does not convey information about reliability, but only about the state of a system. Hence, this justifies naming η as a non-probabilistic limit-state measure.

Meanwhile, as discussed in last section, with the same lower and upper boundary values of interval variables, the value of η^{HR} is smaller than η^{HE}, which indicates that the HE model is more optimistic than the HR model, where the potential degree of over-conservatism of the interval model depends on the dependence between the individual quantities that is assumed to be non-existent in the interval model. Irrespective of this observation, the non-probability limit-state measure η can be used as an informative quantity characterizing the safety of a system subject to epistemic uncertainty. In addition, if an uncertain input variable has a significant impact on η, it indicates that this variable also has a significant impact on the overall behaviour of the system. In the next section, a sensitivity analysis based on the concept of η is conducted.

A proposed sensitivity index and its computational strategy

As discussed in last section, the non-probabilistic limit-state measure η value is informative on the state of the structure. In this section, the sensitivity analysis based on the concept of η is considered, and a new sensitivity index is proposed. The proposed sensitivity index quantifies the influence degree of each interval input variable (or a subset of interval variables) on the state of the structure. Finally, the related characteristics and a computational strategy of the proposed sensitivity index are discussed in detail.

Proposed sensitivity index based on non-probabilistic limit-state measure

Taking the hyper-rectangle model as an example to illustrate the proposed sensitivity index, suppose that the variable X_i is fixed at a nominal value within its associated domain (e.g., $X_i = x_i$) and all other variables still vary within the n-1 dimensional variable space $\{\boldsymbol{X}_{\sim i} : \left|\boldsymbol{X}_{\sim i} - \boldsymbol{X}_{\sim i}^c\right| \leqslant \boldsymbol{X}_{\sim i}^r\}$, where $\sim i$ denotes the other elements expect for the i-th element, thus $\boldsymbol{X}_{\sim i} = [X_1, ..., X_{i-1}, X_{i+1} ..., X_n]$ denotes the interval vector associated with all variables expect X_i. According to Eq.(8), the conditional limit-state measure $\eta_i(X_i)$ with X_i fixed at its nominal value is calculated as

$$\eta_i(X_i) = \frac{M_i^c}{M_i^r} \tag{11}$$

where M_i^c and M_i^r denote the centre value and radius of the interval of conditional state function M_i^I, respectively. Eq.(11) shows that when X_i takes different nominal values within its corresponding interval X_i^I, the conditional non-probabilistic limit-state measure $\eta_i(X_i)$ will also take different values within an interval, that is, $\eta_i^I = [\eta_i^L, \eta_i^U]$, where η_i^L denotes the lower bound and η_i^U denotes the upper bound of the interval of conditional limit-state measure η_i^I. The illustration of this interval η_i^I in the original variable space and in the standard variable space is shown in Figure 4.

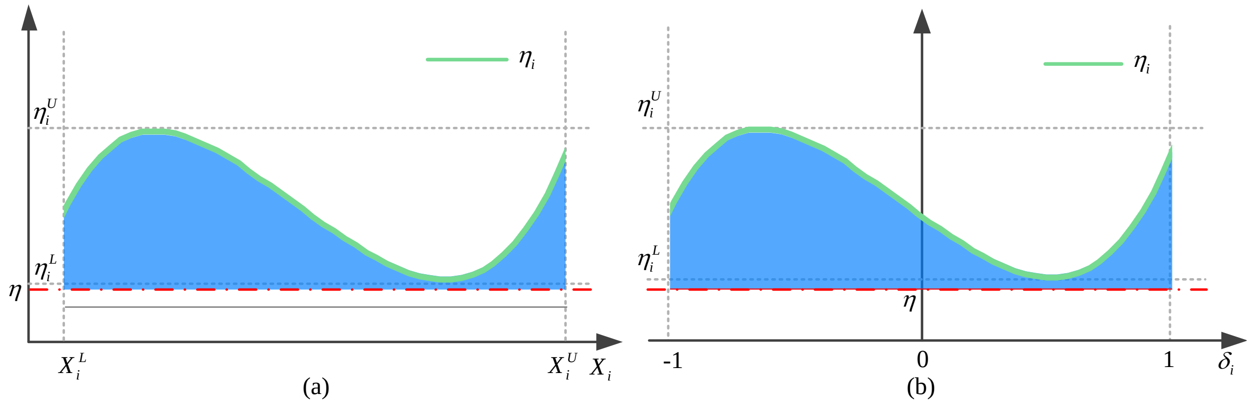

Figure 4 Illustration of the interval of the conditional non-probabilistic state measure in (a) the original space and in (b) the standardized space

It is clear that $\eta_i(X_i)$ changes as X_i takes different nominal values, indicating that the limit-state measure of the structure changes as well. Since X_i is fixed at its nominal value, the effect of the uncertainty of X_i on the non-probabilistic limit-state measure can be evaluated. In fact, the difference between $\eta_i(X_i)$ and η should be able to effectively reflect the influence of X_i on the state of system (Chang et al. 2022). Thus, a new sensitivity index based on the non-probabilistic limit-state measure is defined as follows:

$$\lambda_i = A(\eta_i(X_i), \eta) \tag{12}$$

where $A(\eta_i, \eta)$ denotes the area (represented by the blue shaded area in Figure 4) enclosed by conditional limit-state measure $\eta_i(X_i)$ and η. The proposed sensitivity index λ_i is defined then as:

$$\lambda_i = \int_{-1}^{1} \left(\eta_i(\delta_i) - \eta\right) \mathrm{d}\delta_i \tag{13}$$

This proposed sensitivity index λ_i comprehensively quantifies the difference between $\eta_i(X_i)$ and η, thus revealing the impact of variable X_i on the state of system. Furthermore, when we intend to determine the joint impact of two variables X_i and X_j on the system's state, the proposed sensitivity index can be further extended as follows:

$$\lambda_{i,j} = A(\eta_{i,j}, \eta) \tag{14}$$

where $\eta_{i,j}(X_i, X_j)$ denotes the non-probabilistic state measure when X_i and X_j take nominal values.

Referring to Eq.(13), an integral for calculating $\lambda_{i,j}$ can be also obtained as follows:

$$\lambda_{i,j} = \int_{-1}^{1}\int_{-1}^{1}\left(\eta_{i,j}(\delta_i,\delta_j) - \eta\right)\mathrm{d}\delta_i \mathrm{d}\delta_j \tag{15}$$

Furthermore, the joint impact on reliability between *m* variables $(X_i, X_j, \cdots, X_k)$ can be obtained by considering multiple integrals as follows:

$$\lambda_{i,j,\cdots,k} = \int_{-1}^{1}\cdots\int_{-1}^{1}\int_{-1}^{1}\left(\eta_{i,j,\cdots,k}(\delta_i,\delta_j,\cdots,\delta_k) - \eta\right)\mathrm{d}\delta_i \mathrm{d}\delta_j \cdots \mathrm{d}\delta_k \tag{16}$$

The above definition of the proposed new sensitivity index does not involve taking into account possible dependences between variables; thus, the proposed sensitivity index can be easily extended to the hyper-ellipsoid model.

Characteristics of the proposed sensitivity index

According to the definition of the proposed sensitivity index, the following properties can be derived.

Property 1: $\lambda_i \geq 0$: The proposed sensitivity index λ_i is the area enclosed by a curve $\eta_i(X_i)$ and a straight line η. Therefore, the lower bound of λ_i is 0.

Property 2: If $\lambda_i = 0$, X_i has no effect on the non-probabilistic limit-state measure.

Property 3: If $\lambda_i > \lambda_j$, X_i has a greater impact on the limit-state measure compared to X_j.

Property 4: If X_i influences state of the system but X_j has no influence, then $\lambda_{i,j} = \lambda_i$.

The proposed sensitivity index λ_i measures the effect of the variables on the non-probabilistic limit-state measure by considering the difference of the interval-valued process associated with the conditional non-probabilistic limit-state measure $\eta_i(X_i)$ with respect to η. The above characteristics will be further explained through examples in next Section.

A computational strategy for calculating the proposed sensitivity index

From the definition of η in Eq.(8), regardless of the interval model or hyper-ellipsoid model, the value of η can be obtained by solving the upper and lower bounds of the performance function response, i.e.,

$$\eta = \frac{M^c}{M^r} = \frac{M^U + M^L}{M^U - M^L} \tag{17}$$

Therefore, the conditional non-probabilistic limit-state measure $\eta_i(X_i)$ can also be obtained by solving the upper and lower bounds of the conditional performance function response, i.e.,

$$\eta_i(X_i)=\frac{M_i^c}{M_i^r}=\frac{M_i^U(X_i)+M_i^L(X_i)}{M_i^U(X_i)-M_i^L(X_i)} \tag{18}$$

Then, the proposed sensitivity index λ_i can be obtained by calculating the area enclosed by η and $\eta_i(X_i)$. Thus, the key to calculating λ_i is to obtain M^U, M^L, $M_i^U(X_i)$ and $M_i^L(X_i)$. Actually, the calculation of these quantities corresponds to a classical interval analysis problem, which has been discussed in detail, for example, by Faes and Moens (Faes and Moens 2020) . In our work, the following optimization models are used to calculate these quantities:

$$\begin{aligned}&\text{Find} \quad \boldsymbol{X}^*=[X_1^*,X_2^*,\dots,X_n^*]\\&\text{to minimize} \quad M=G(\boldsymbol{X})\\&\text{subject to} \quad \boldsymbol{X}\in\{|\boldsymbol{X}-\boldsymbol{X}^c|\le\boldsymbol{X}^r\}\end{aligned} \tag{19}$$

and

$$\begin{aligned}&\text{Find} \quad \boldsymbol{X}^{**}=[X_1^{**},X_2^{**},\dots,X_n^{**}]\\&\text{to maximize} \quad M=G(\boldsymbol{X})\\&\text{subject to} \quad \boldsymbol{X}\in\{|\boldsymbol{X}-\boldsymbol{X}^c|\le\boldsymbol{X}^r\}\end{aligned} \tag{20}$$

By fixing variable X_i at its nominal value x_i, $M_i^U(X_i)$ and $M_i^L(X_i)$ can be obtained by solving the following optimization problems:

$$\begin{aligned}&\text{Find} \quad \boldsymbol{X}_{\sim i}^*=[X_1^*,\dots,x_i,\dots,X_n^*]\\&\text{to minimize} \quad M_i=G(\boldsymbol{X}_{\sim i},x_i)\\&\text{subject to} \quad \boldsymbol{X}_{\sim i}\in\{|\boldsymbol{X}_{\sim i}-\boldsymbol{X}_{\sim i}^c|\le\boldsymbol{X}_{\sim i}^r\}\end{aligned} \tag{21}$$

and

$$\begin{aligned}&\text{Find} \quad \boldsymbol{X}_{\sim i}^{**}=[X_1^{**},\dots,x_i,\dots,X_n^{**}]\\&\text{to maximize} \quad M_i=G(\boldsymbol{X}_{\sim i},x_i)\\&\text{subject to} \quad \boldsymbol{X}_{\sim i}\in\{|\boldsymbol{X}_{\sim i}-\boldsymbol{X}_{\sim i}^c|\le\boldsymbol{X}_{\sim i}^r\}\end{aligned} \tag{22}$$

Eq.(19) and Eq.(20) provides the solution of M^U and M^L. By fixing the variable X_i at its nominal value x_i, $M_i^U(X_i)$ and $M_i^L(X_i)$ are solved by Eq.(21) and Eq.(22), respectively. In this work, a surrogate optimization algorithm is adopted to obtain these quantities (Regis and Shoemaker 2007).

As defined in Eq.(13), the calculation of the proposed sensitivity index x_i requires the maximum and minimum values of the conditional performance function X_i^I at each nominal value x_i within the variable interval X_i^I. If the variable interval X_i^I is directly discretized for calculation, the calculation accuracy cannot be guaranteed when there are too few discrete points. However, when there are too many discrete points, the calculation cost will be increased significantly. Thus, the Kriging surrogate model, which can approximate the relationship between the variable X_i and its corresponding maximum or minimum values of the conditional performance function, is introduced in this work. To reduce the number of calls to the performance function while ensuring the accuracy of the Kriging surrogate model, an adaptive learning method is also introduced.

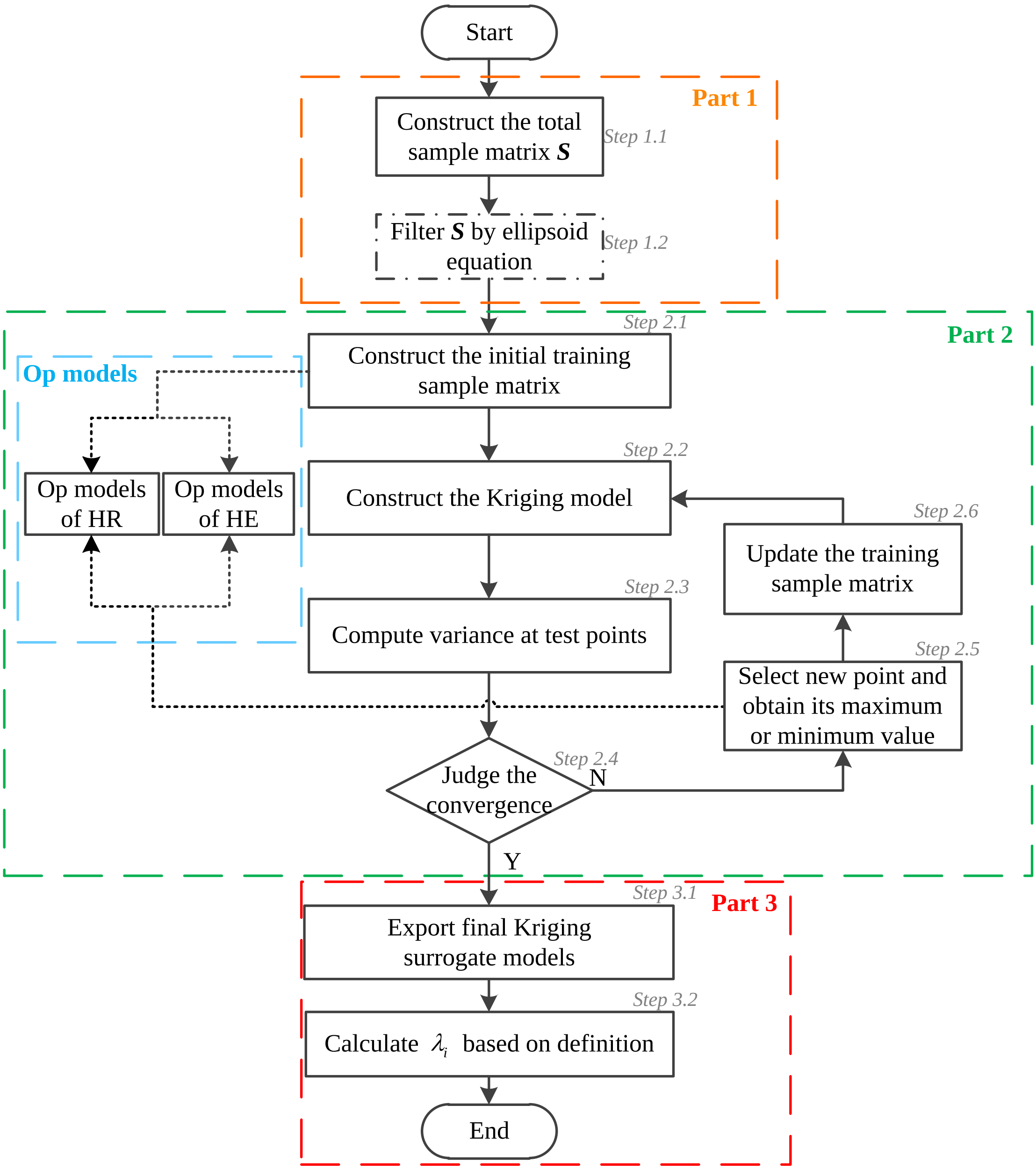

Figure 5 Flow chart of the proposed computation strategy.

The basic procedure of the computational strategy is depicted in Figure 5, and the details are given as follows.

Part 1: Pre-treatment process

Step 1.1: Construct the total sample matrix $\boldsymbol{S}$.

Apply the Latin hypercube sampling (LHS) or Sobol sampling method to obtain N samples of the uncertain input parameters. These samples are stored in matrix $\boldsymbol{S}=\begin{bmatrix} x_1^{(1)} & \dots & x_i^{(1)} & \dots & x_n^{(1)} \\ \vdots & \vdots & \vdots & \vdots & \vdots \\ x_1^{(N)} & \dots & x_i^{(N)} & \dots & x_n^{(N)} \end{bmatrix}$ (Liu et al. 2018). Please note that in this step, none of the sample points are evaluated by calling the performance function.

Step 1.2: Filter sample matrix $\boldsymbol{S}$ in case that the hyper-ellipsoid model is considered.

If dependence between variables is considered, i.e., using the hyper-ellipsoid model or a hybrid model (that is, interval and hyper-ellipsoid models co-exist simultaneously) to describe the uncertainty of the input variables, the total sample matrix $\boldsymbol{S}$ obtained in the previous step should be filtered by the ellipsoid equation. That is, the sample points located outside the area defined by the ellipsoid equation are excluded.

Part 2: Construction of the adaptive Kriging surrogate model

Step 2.1: Construct the initial training sample matrix.

Randomly select samples from $\boldsymbol{S}$ to form the initial sample matrix $\boldsymbol{S}=\begin{bmatrix} x_1^{(1)} & \dots & x_i^{(1)} & \dots & x_n^{(1)} \\ \vdots & \vdots & \vdots & \vdots & \vdots \\ x_1^{(N_0)} & \dots & x_i^{(N_0)} & \dots & x_n^{(N_0)} \end{bmatrix}$, where N_0 denotes the number of initial sample points. Based on the optimization problems shown in Eq.(21) and Eq.(22) and the *i*-th column sample points $[x_i^{(1)},...,x_i^{(N_0)}]^{\mathrm{T}}$ of $\boldsymbol{S}_0$, obtain the corresponding maximum values $[M_i^{U(1)},...,M_i^{U(N_0)}]^{\mathrm{T}}$ and minimum values $[M_i^{L(1)},...,M_i^{L(N_0)}]^{\mathrm{T}}$ of the conditional performance function $M_i=G(\boldsymbol{X}_{\sim i},x_i)$ by solving the following optimization problems for $j=1,...,N_0$,

$$\begin{array}{l} \text{Find} \quad \boldsymbol{X}_{\sim i}^{*(j)}=[X_1^{*(j)},...,x_i^{(j)},...,X_n^{*(j)}] \\ \text{to minimize} \quad M_i^{L(j)}=G(\boldsymbol{X}_{\sim i},x_i^{(j)}) \\ \text{subject to} \begin{cases} \boldsymbol{X}_{\sim i}\in\{\boldsymbol{X}:\left|\boldsymbol{X}_{\sim i}-\boldsymbol{X}_{\sim i}^{c}\right|\le\boldsymbol{X}_{\sim i}^{r}\} & \text{in case of the HR model} \\ \boldsymbol{X}_{\sim i}\in\left\{\boldsymbol{X}:(\boldsymbol{X}_{\sim i}-\boldsymbol{X}_{\sim i}^{c})^{T}\boldsymbol{W}(\boldsymbol{X}_{\sim i}-\boldsymbol{X}_{\sim i}^{c})\le\theta^2\right\} & \text{in case of the HE model} \end{cases} \end{array} \tag{23}$$

and

$$\begin{array}{l} \text{Find} \quad \boldsymbol{X}_{\sim i}^{**(j)}=[X_1^{**(j)},...,x_i^{(j)},...,X_n^{**(j)}] \\ \text{to maximize} \quad M_i^{U(j)}=G(\boldsymbol{X}_{\sim i},x_i^{(j)}) \\ \text{subject to} \begin{cases} \boldsymbol{X}_{\sim i}\in\{\boldsymbol{X}:\left|\boldsymbol{X}_{\sim i}-\boldsymbol{X}_{\sim i}^{c}\right|\le\boldsymbol{X}_{\sim i}^{r}\} & \text{in case of the HR model} \\ \boldsymbol{X}_{\sim i}\in\left\{\boldsymbol{X}:(\boldsymbol{X}_{\sim i}-\boldsymbol{X}_{\sim i}^{c})^{T}\boldsymbol{W}(\boldsymbol{X}_{\sim i}-\boldsymbol{X}_{\sim i}^{c})\le\theta^2\right\} & \text{in case of the HE model} \end{cases} \end{array} \tag{24}$$

Based on the above results, construct the initial training sample matrix $\boldsymbol{S}_0^i=\begin{bmatrix} x_i^{(1)} & M_i^{U(1)} & M_i^{L(1)} \\ \vdots & \vdots & \vdots \\ x_i^{(N_0)} & M_i^{U(N_0)} & M_i^{L(N_0)} \end{bmatrix}$.

Step 2.2: Construct the Kriging surrogate models between the variable X_i and the maximum or minimum value of the conditional performance function.

Two Kriging surrogate models are established based on the initial training sample matrix $\boldsymbol{S}_0^i$ obtained in **Step 2.1:** one for the minimum value and another one for the maximum value. The Gaussian form dependence function (also known as the Gaussian form kernel function) is selected here, and this step is performed with the toolbox DACE (Lophaven et al. 2002).

Step 2.3: Compute variance at test points of total sample pool $\boldsymbol{S}$.

Based on the constructed Kriging surrogate model in the last step, compute the Kriging prediction variance σ_K^2 for each point in the *i*-th column of the total sample pool $\boldsymbol{S}$.

Step 2.4: Judge the convergence of the adaptive Kriging surrogate model.

The convergence criterion can be implemented by setting a maximum value of the Kriging prediction variance (i.e., max $\sigma_K^2(X_i) \le \sigma_K^{2*}$) or by setting a maximum number of model calls (Liu et al. 2018). In this work, the construction of the adaptive Kriging surrogate model is stopped when either of the two criterion is satisfied. If the convergence criterion is not met, then go to **Step 2.5**; otherwise, go to **Step 3.1**.

Step 2.5: Select new point x_i^{new} and obtain its corresponding maximum or minimum value.

The point with the maximum prediction variance value associated with the *i*-th column of the total sample pool $\boldsymbol{S}$ is selected as the best new point x_i^{new}, i.e.,

$$x_i^{new} = \arg\max_{X_i \in \boldsymbol{S}} \sigma_K^2(X_i) \tag{25}$$

Based on the selected new point x_i^{new} by the maximum variance criterion, apply the optimization models to obtain the maximum or minimum value, and the optimization models are denoted as follows:

$$\begin{aligned}
&\text{Find} \quad \boldsymbol{X}_{\sim i}^{*} = [X_1^{*}, ..., x_i^{new}, ..., X_n^{*}] \\
&\text{to minimize} \quad M_i^{L(new)} = G(\boldsymbol{X}_{\sim i}, x_i^{new}) \\
&\text{subject to} \begin{cases} \boldsymbol{X}_{\sim i} \in \{\boldsymbol{X} : \left|\boldsymbol{X}_{\sim i} - \boldsymbol{X}_{\sim i}^{c}\right| \le \boldsymbol{X}_{\sim i}^{r}\} & \text{in case of the HR model} \\ \boldsymbol{X}_{\sim i} \in \left\{\boldsymbol{X} : (\boldsymbol{X}_{\sim i} - \boldsymbol{X}_{\sim i}^{c})^{T} \boldsymbol{W} (\boldsymbol{X}_{\sim i} - \boldsymbol{X}_{\sim i}^{c}) \le \theta^2 \right\} & \text{in case of the HE model} \end{cases}
\end{aligned} \tag{26}$$

and

$$\begin{aligned}
&\text{Find} \quad \boldsymbol{X}_{\sim i}^{**} = [X_1^{**}, ..., x_i^{new}, ..., X_n^{**}] \\
&\text{to maximize} \quad M_i^{U(new)} = G(\boldsymbol{X}_{\sim i}, x_i^{new}) \\
&\text{subject to} \begin{cases} \boldsymbol{X}_{\sim i} \in \{\boldsymbol{X} : \left|\boldsymbol{X}_{\sim i} - \boldsymbol{X}_{\sim i}^{c}\right| \le \boldsymbol{X}_{\sim i}^{r}\} & \text{in case of the HR model} \\ \boldsymbol{X}_{\sim i} \in \left\{\boldsymbol{X} : (\boldsymbol{X}_{\sim i} - \boldsymbol{X}_{\sim i}^{c})^{T} \boldsymbol{W} (\boldsymbol{X}_{\sim i} - \boldsymbol{X}_{\sim i}^{c}) \le \theta^2 \right\} & \text{in case of the HE model} \end{cases}
\end{aligned} \tag{27}$$

Step 2.6: Update the training sample matrix $\boldsymbol{S}_0^i$.

Based on the adaptively selected new point and its corresponding maximum and minimum value, i.e., $[x_i^{new}, M_i^{L(new)}]$ and $[x_i^{new}, M_i^{U(new)}]$, respectively, update the training sample matrix $\boldsymbol{S}_0^i$. Then, return to **Step 2.2** to reconstruct the Kriging surrogate model with the updated sample matrix $\boldsymbol{S}_0^i$.

Part 3: Sensitivity index calculation

Step 3.1: Export the final Kriging surrogate models.

The Kriging surrogate models of the variable X_i with lower and upper bounds of the conditional performance function are exported for further sensitivity index calculation.

Step 3.2: Calculate the proposed sensitivity index λ_i.

As discussed in previous section, an integral form of the proposed sensitivity index is denoted by Eq.(13). Thus, based on the obtained Kriging surrogate model of the lower and upper bounds of the conditional performance function, a numerical integration method of approximating an integral using the sum of a series of rectangles is selected to calculate the proposed sensitivity index λ_i which can be easily derived as follows,

$$\lambda_i = \lim_{h_k \to 0} \sum_{k=1}^{m} |\eta_i(\delta_k) - \eta| h_k \approx \Delta h \bullet \sum_{k=1}^{m} |\eta_i(\delta_k) - \eta| \tag{28}$$

where $\Delta h = \delta_{k+1} - \delta_k$ denotes the width of a rectangle and $\Delta h = 0.001$ is selected in this paper. The integrand part $|\eta_i(\delta_k) - \eta|$ denotes the length of a rectangle which can be estimated based on the Kriging surrogate model.

The algorithm described above consists of a double-loop strategy to solve the proposed sensitivity index λ_i. To calculate all sensitivity indexes, the strategy must be repeated for each X_i. The proposed algorithm is composed of three parts, i.e., Part 1: pre-treatment process, Part 2: construction of the adaptive Kriging surrogate model and optimization and Part 3: sensitivity index calculation. The computational cost of the proposed index mainly comes from Part 2, which needs multiple calls to the original performance function. And in the construction process of Kriging model, because both the dimension of input and output are one-dimensional variables, generally, a reduced number of samples can meet the convergence criterion of the adaptive learning process. By filtering samples and introducing the hyper-ellipsoid model in the optimization problems, the universality of the proposed algorithm has been enhanced. The proposed algorithm is applicable not only to the hyper-rectangular model but also to the hyper-ellipsoid model or a more general hybrid model.

Numerical examples

To illustrate the effectiveness of the proposed sensitivity index associated with the non-probabilistic state measure, two numerical examples are considered in this section. For comparison, two sensitivity indices proposed by Li et al. (Li et al. 2013) are also considered in this work. These indexes are defined based on the conditional non-probabilistic limit-state measure $\eta_i(X_i)$ (see Eq.(18)) as:

$$\varepsilon_i = \frac{\eta_i^r}{\eta}, \tag{29}$$

and

$$\xi_i = \left|\frac{\eta - \eta_i^c}{\eta}\right|, \tag{30}$$

where $\eta_i^r(X_i) = \dfrac{\eta_i^U(X_i) - \eta_i^L(X_i)}{2}$ denotes the radius of $\eta_i(X_i)$ and $\eta_i^c(X_i) = \dfrac{\eta_i^U(X_i) + \eta_i^L(X_i)}{2}$ denotes the centre value of $\eta_i(X_i)$. The above two indices are called the shape effect index ε_i and the position effect index ξ_i, respectively. From the above definitions, note that the radius $\eta_i^r(X_i)$ reflects the shape of the interval associated with $\eta_i(X_i)$; thus, the index ε_i is called the shape effect index. The centre value $\eta_i^c(X_i)$ reflects the position of the interval of $\eta_i(X_i)$; thus, the index ξ_i is called the position effect index. The geometrical illustrations of ε_i and ξ_i are shown in Figure 6. The proposed computational strategy can also be used to calculate these two indices.

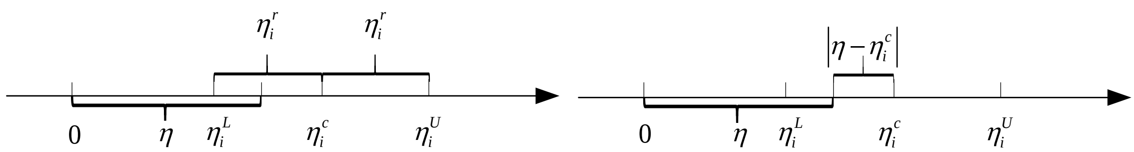

(a) The shape effect index ε_i (b) The position effect index ξ_i

Figure 6 The geometric meaning of the two sensitivity indices ε_i and ξ_i

Example 1: Linear numerical example

The performance function is defined as (Li et al. 2013)

$$G(\boldsymbol{X}) = X_1 + 1/\sqrt{2}\,X_2 - X_3, \tag{31}$$

where $\boldsymbol{X} \in \boldsymbol{X}^I = [X_1^I, X_2^I, X_3^I]$ are the interval variables with centre value $\boldsymbol{X}^c = [200, 300, 200]$ and radius

$\boldsymbol{X}^r = [20,30,40]$. The lower and upper bounds are $\boldsymbol{X}^L = [180,270,160]$ and $\boldsymbol{X}^U = [220,330,240]$, respectively. When the variables in $\boldsymbol{X}$ are independent, only the lower and upper bounds are given. When X_1 and X_2 are dependent, the elliptic model characterizing the relationship between X_1 and X_2 is further described as

$$\frac{(X_1 - X_1^c)^2}{(X_1^r)^2} + \frac{(X_2 - X_2^c)^2}{(X_2^r)^2} \leq 1 \tag{32}$$

Based on the above contents, the conditional (denoted by the green line) and unconditional (denoted by the red line) non-probabilistic limit-state measures for the two cases are depicted in Figure 7 **错误!未找到引用源。**.

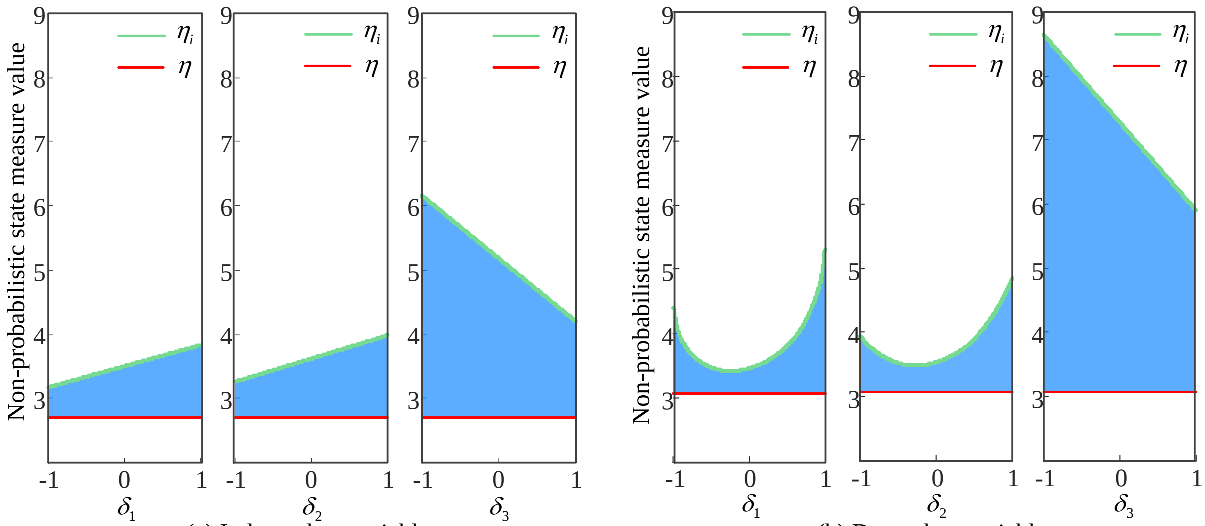

(a) Independent variables (b) Dependent variables

Figure 7 The change trend of the conditional non-probabilistic limit-state measure for Example 1

Table 1 The results of three types of indices of Example 1 with independent variables

Variables	η_i^L	η_i^U	Sensitivity indices		
			ξ_i	ε_i	λ_i
X_1	3.139	3.792	0.327(3)	0.125(3)	1.707(3)
X_2	3.182	3.889	0.354(2)	0.135(2)	1.847(2)
X_3	4.177	6.118	0.971(1)	0.372(1)	5.070(1)

[a]The superscripts of index results are the sensitivity ranking from highest to lowest.

In the case of independent variables in Figure 7 (a), the relationship between the conditional performance measure $\eta_i(X_i)$ and the variables is monotonic. In the case of dependent variables shown in Figure 7 (b), there is a nonmonotonic situation related to X_1 and X_2 due to the existence of dependence. Meanwhile, the blue area enclosed by conditional and unconditional non-probabilistic probabilistic measures is changed compared with the case of independent variables. The reason for this situation is that the uncertainty space of X_1 and X_2 has changed from a rectangle to an ellipse. For the same reason, for X_3, the monotonic relationship still exists, but the value of $\eta_i(X_i)$ in the dependent case is larger than the value in the independent case for different nominal values. To quantify the above changes, further sensitivity analysis was applied.

Table 2 The results of three types of indices of Example 1 with dependent variables

Variables	η_i^L	η_i^U	Sensitivity indices		
			ξ_i	ε_i	λ_i
X_1	3.502	5.048	0.394(2)	0.278(2)	1.400(3)
X_2	3.475	5.021	0.385(3)	0.252(3)	1.507(2)
X_3	5.895	8.649	1.371(1)	0.449(1)	8.411(1)

By applying the proposed computational strategy, the results of three types of sensitivity indices are obtained in Table 1 and Table 2. In the case of independent variables, the values of the three types of sensitivity indices of X_3 are the maximum, as shown in Table 1. According to the discussions in previous section, X_3 has the most impact on performance. In the case of dependent variables, X_3 still holds the first place of impact on performance according to the results of three sensitivity indices, as shown in Table 2. It can be seen from the degree of change in the value of the three indices that the impact on the performance of X_3 has been further increased. Thus, when the dependence between X_1 and X_2 is considered, X_3 still has the greatest impact on reliability, and its importance is further increased compared with the independent case. The remaining variables X_1 and X_2 have no significant difference in the impact on the state of performance function. In addition, from the comparison of three sensitivity indices results from Table 1 and Table 2, after the dependence is considered, the increase in the value of the proposed sensitivity index is greater than other two indices. Based on the definitions of these three sensitivity indices, we can draw a conclusion that the proposed sensitivity index can effectively identify an important input variable not only from radius or median value of non-probabilistic limit-state measure, but also from the interval areas that cannot be covered by Li's sensitivity indices (Li et al. 2013). Thus, the proposed sensitivity index can provide more comprehensive results especially after the dependence is considered.

Example 2: Ishigami function

The Ishigami function is frequently used to study uncertainty quantification, and the performance function is defined as (Chang et al. 2022)

$$G(\boldsymbol{X}) = \sin(X_1) + a\sin^2(X_2) + bX_3^4\sin(X_1) \tag{33}$$

where $\boldsymbol{X} \in \boldsymbol{X}^I = [X_1^I, X_2^I, X_3^I]$ are interval variables with centre value $\boldsymbol{X}^c = [\pi/2, \pi/2, \pi/2]$ and radius $\boldsymbol{X}^r = [\pi/4, \pi/4, \pi/4]$, and $a = 5$, $b = 0.1$. When the variables $\boldsymbol{X}$ are independent, only the lower and upper bounds are given. When X_1 and X_3 are dependent, the elliptic function that describes the relationship between X_1 and X_3 is further denoted as

$$\frac{(X_1 - X_1^c)^2}{(X_1^r)^2} + \frac{(X_3 - X_3^c)^2}{(X_3^r)^2} \le 1 \tag{34}$$

Based on the above contents, the conditional (denoted by the green line) and unconditional (denoted by the red line) non-probabilistic limit-state measure for the two cases are depicted in Figure 8.

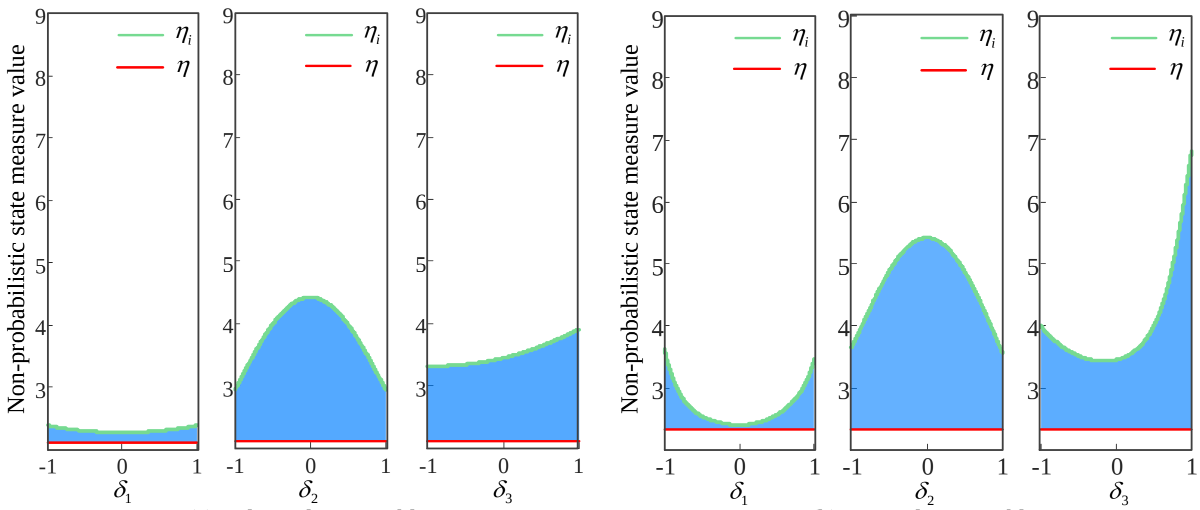

(a) Independent variables (b) Dependent variables

Figure 8 The change trend of the conditional non-probabilistic limit-state measure for Example 2

In the case of independent variables (shown in Figure 8 (a)), the nonlinearity of the performance function induces nonlinearity between the conditional non-probabilistic limit-state measure $\eta_i(X_i)$ and the variable. In the case of dependent variables (shown in Figure 8 (b)), the curves of conditional non-probabilistic limit-state measure $\eta_i(X_i)$ of X_1 and X_3 are concave due to the existence of dependence. When the relevant variable takes the interval boundary value (e.g., δ_1=1 or $X_1 = X_1^U$), the dependence causes the variable space to decrease and the uncertainty to be reduced, resulting in an increase in the non-probabilistic limit-state measure value. For the independent variable X_2 , the curve of the conditional non-probabilistic limit-state measure $\eta_2(X_2)$ becomes more prominent when the dependence between X_1 and X_3 is considered. To quantify the above changes, further sensitivity analysis was applied.

Table 3 The results of three types indices of Example 2 with independent variables

Variables	η_i^L	η_i^U	Sensitivity indices		
			ξ_i	ε_i	λ_i
X_1	2.276	2.390	0.108[(3)]	0.027[(3)]	0.413[(3)]
X_2	2.932	4.425	0.747[(1)]	0.355[(1)]	3.553[(1)]
X_3	3.307	3.915	0.715[(2)]	0.144[(2)]	2.798[(2)]

Table 4 The results of three types indices of Example 2 with dependent variables

Variables	η_i^L	η_i^U	Sensitivity indices		
			ξ_i	ε_i	λ_i
X_1	2.279	3.417	0.288[(3)]	0.257[(3)]	0.699[(3)]
X_2	3.170	4.754	0.792[(2)]	0.358[(2)]	3.935[(1)]
X_3	3.422	6.237	1.184[(1)]	0.637[(1)]	3.285[(2)]

By applying the proposed computational strategy, the results of three types of sensitivity indices are obtained in Table 3 and Table 4. In the case of independent variables, the values of three types of sensitivity indices associated with X_2 contain the maximum value, as shown in Table 3. The three sensitivity index rankings obtained are consistent with each other, that is, $\xi_2 > \xi_3 > \xi_1$, $\varepsilon_2 > \varepsilon_3 > \varepsilon_1$, and $\lambda_2 > \lambda_3 > \lambda_1$. According to the previous discussion, X_2 has the greatest impact on structural reliability. By comparing the calculation results of the lower and upper bounds of conditional non-probabilistic limit-state measure $\eta_i(X_i)$ in Table 3 and Table 4, it is clear that there are significant differences due to the existence of a dependence between X_1 and X_3. Especially the value of η_3^U has a significant change. As we discussed in Example 1, these two sensitivity indices proposed by Li et al (Li et al. 2013) rely on radius or median values, which are determined by the lower and upper bounds of $\eta_i(X_i)$. Thus, the importance ranking measured by the two sensitivity indices has changed to $\xi_3 > \xi_2 > \xi_1$, $\varepsilon_3 > \varepsilon_2 > \varepsilon_1$. But X_2 still holds the first place of impact on structure performance according to the results of the proposed sensitivity index λ_i, as shown in Table 4. The proposed sensitivity index λ_i is more inclined to quantify the changes of non-probabilistic state measure from the perspective of the entire interval space and may conclude different sensitivity analysis results compared with the existing sensitivity indices.

Application to the honeycomb sandwich radome structure

The radome structure can provide protection for aircraft radar antenna systems in harsh environments, preventing radar system failures caused by lightning strikes, hail, wind pressure, and other environmental factors, as well as serious flight accidents (Zhou et al. 2021a). Therefore, ensuring the stability and reliability of radome structures is of great significance.

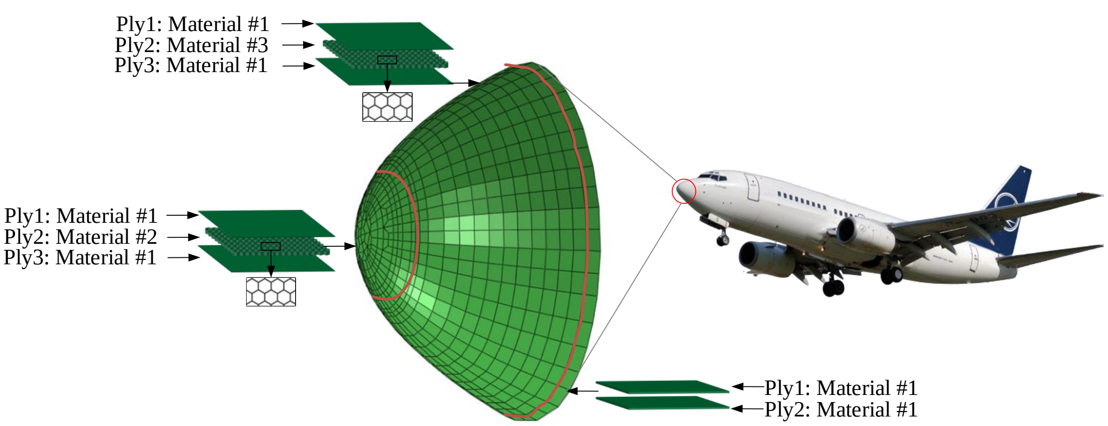

Figure 9 Radome parts and their material assembly

The honeycomb sandwich radome structure studied in this work is composed of three parts (divided by red line): Parts #1, #2 and #3. Three types of materials are used: Material #1 denotes a type of composite laminate, Material #2 denotes the flexible honeycomb core, and Material #3 denotes the hexagonal honeycomb core. The finite element model of the radome structure and the materials used in each ply are shown in Figure 9. Three types of variables (i.e., elastic modulus, density, and thickness) are considered interval variables, and the corresponding information is shown in Table 5. Based on two structure response outputs, including the maximum displacement Y and total strain energy E, two performance functions are constructed as

$$G^D(\boldsymbol{X}) = D^* - D(\boldsymbol{X}) \tag{35}$$

$$G^E(\boldsymbol{X}) = E^* - E(\boldsymbol{X}) \tag{36}$$

where D^* and E^* represent the threshold of the maximum displacement and the total strain energy, respectively.

Table 5 Information on the variables of the radome structure

Variables	Symbol	Meaning of the variables	Intervals of the variables
X_1	Mat_1E_{11}	Elastic modulus in 11 direction of material #1	$[1.24\times10^{10}, 1.86\times10^{10}]$ Pa
X_2	Mat_1E_{22}	Elastic modulus in 22 direction of material #1	$[1.24\times10^{10}, 1.86\times10^{10}]$ Pa
X_3	Mat_1G_{12}	Elastic modulus in 12 direction of material #1	$[5.84\times10^{9}, 8.76\times10^{9}]$ Pa
X_4	Mat_1G_{13}	Elastic modulus in 13 direction of material #1	$[2.88\times10^{9}, 4.32\times10^{9}]$ Pa
X_5	Mat_1G_{23}	Elastic modulus in 23 direction of material #1	$[2.88\times10^{9}, 4.32\times10^{9}]$ Pa
X_6	Mat_1Rho	Density of material #1	[1462.4, 2193.6] kg/m^3
X_7	Mat_2E_{11}	Elastic modulus in 11 direction of material #1	$[3.6\times10^{4}, 5.4\times10^{4}]$ Pa
X_8	Mat_2E_{22}	Elastic modulus in 11 direction of material #1	$[3.6\times10^{4}, 5.4\times10^{4}]$ Pa
X_9	Mat_2G_{12}	Elastic modulus in 11 direction of material #1	$[1.68\times10^{4}, 2.52\times10^{4}]$ Pa
X_{10}	Mat_2G_{13}	Elastic modulus in 11 direction of material #1	$[3.06\times10^{7}, 4.6\times10^{7}]$ Pa

X_{11}	Mat_2G_{23}	Elastic modulus in 11 direction of material #1	[1.5×10^7, 2.24×10^7] Pa
X_{12}	Mat_2Rho	Density of material #2	[52, 78] kg/m^3
X_{13}	Mat_3E_{11}	Elastic modulus in 11 direction of material #1	[3.6×10^6, 5.4×10^6] Pa
X_{14}	Mat_3E_{22}	Elastic modulus in 11 direction of material #1	[3.6×10^6, 5.4×10^6] Pa
X_{15}	Mat_3G_{12}	Elastic modulus in 11 direction of material #1	[3.6×10^6, 5.4×10^6] Pa
X_{16}	Mat_3G_{13}	Elastic modulus in 11 direction of material #1	[1.2×10^7, 1.8×10^7] Pa
X_{17}	Mat_3G_{23}	Elastic modulus in 11 direction of material #1	[2.02×10^7, 3.04×10^7] Pa
X_{18}	Mat_3Rho	Density of material #3	[52, 78] kg/m^3
X_{19}	Th_1	Thickness of Ply 1 and 3 of Part #1 and #2	[6.4×10^-4, 9.6×10^-4] m
X_{20}	Th_2	Thickness of Ply 2 of Part #1 and #2	[4.8×10^-3, 7.2×10^-3] m
X_{21}	Th_3	Thickness of Ply 1 and 2 of Part #3	[2.4×10^-3, 3.6×10^-3] m

The strain energy is the comprehensive embodiment of the mechanical performance of the radome structure. If the displacement exceeds the threshold or the total strain energy is larger than the threshold, the structure will fail. Based on the above assumptions, the proposed solution method is applied to acquire the proposed sensitivity index; meanwhile, the shape effect index and the position effect index (Li et al. 2013) can also be obtained simultaneously.

First, the sensitivity analysis based on the maximum displacement reliability model is discussed. The Kriging surrogate model is applied to estimate the conditional non-probabilistic state measure, as shown in Figure 10. The value of non-probabilistic limit-state measure η is located between 0 and 1 (0.4084, denoted by the red line). According to the discussion about non-probabilistic limit-state measure η, there is a possibility of failure of the radome structure, so it is necessary to identify important variables to improve the performance of the radome structure.

According to the changes in conditional reliability indices in Figure 10, it is evident that except for X_1, X_2 and X_{21}, all other variables have no significant relationship with the changes in reliability indices. The three sensitivity indices are further obtained and shown in Figure 11, which also reveals that under the failure mode of maximum displacement, X_2 has the most significant impact on the limit-state measure of the composite radome structure.

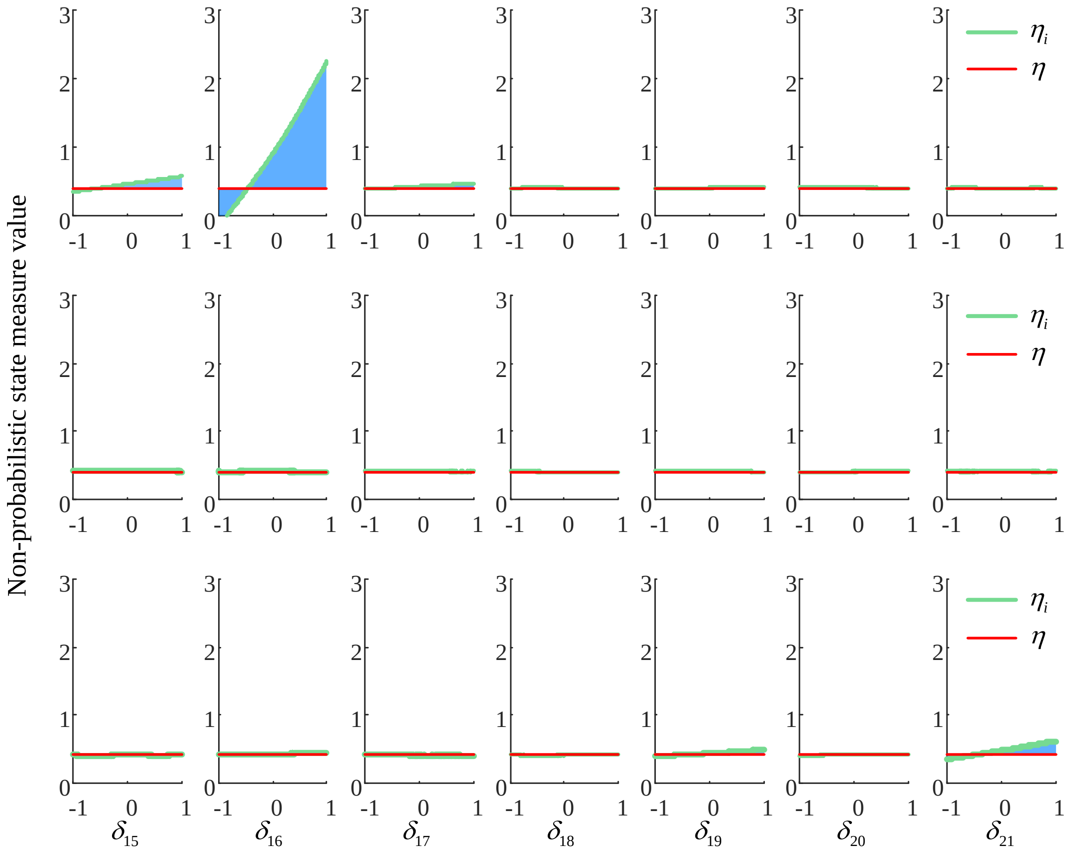

Figure 10 The change trend of the conditional non-probabilistic limit-state measure for maximum displacement

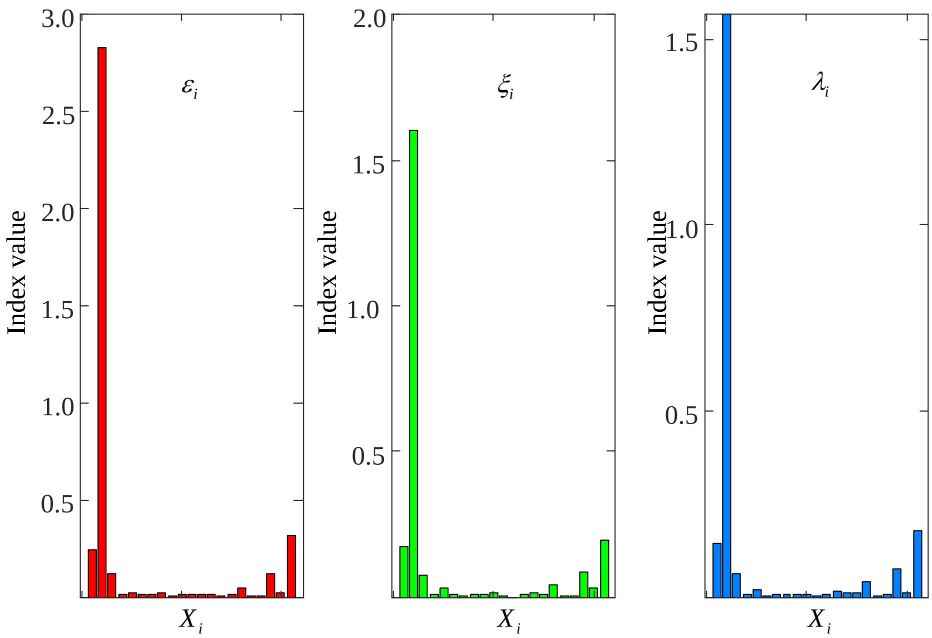

Figure 11 Results of the sensitivity indices of the radome structure in the maximum displacement case

We now discuss the sensitivity analysis based on the total strain energy reliability model. The Kriging surrogate model is applied to estimate the conditional non-probabilistic limit-state measure, as shown in Figure 12. The value of non-probabilistic reliability index η is larger than 1 (2.1087, denoted by the red line). Thus, the radome structure is in a safe state.

However, from the dispersion of the processes of the conditional non-probabilistic limit-state measure $\eta_i(X_i)$, as shown in Figure 12, there are significant fluctuations in the state measure. To quantify these fluctuations, the three sensitivity indices are obtained by the proposed method based on Kriging in Figure 13. Three variables are naturally selected as important variables for the radome structure: X_1 (the elastic modulus in the 11 direction of material #1), X_2 (the elastic modulus in the 22 direction of material #1) and X_{19} (the thickness of Ply1 and 3 of Parts #1 and #2). The identified influential variables can provide design guidance for improving the performance of composite radome structures.

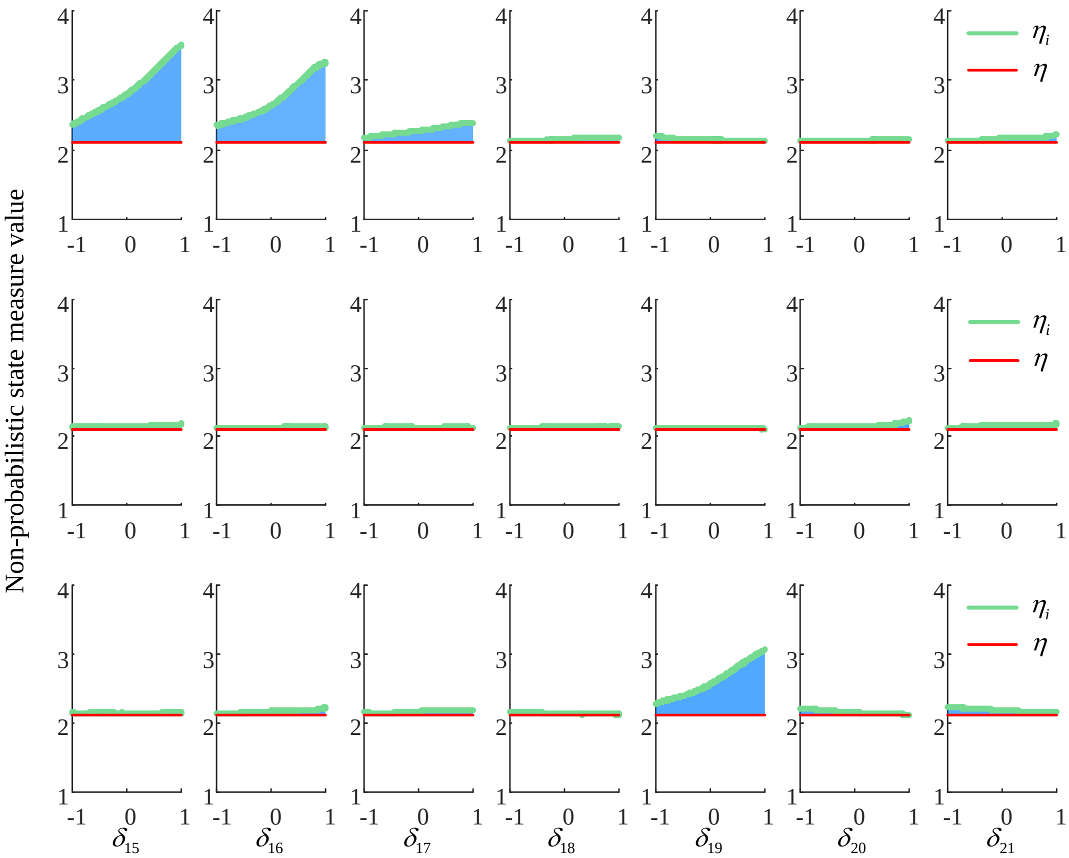

Figure 12 The change trend of the conditional non-probabilistic state measure for total strain energy

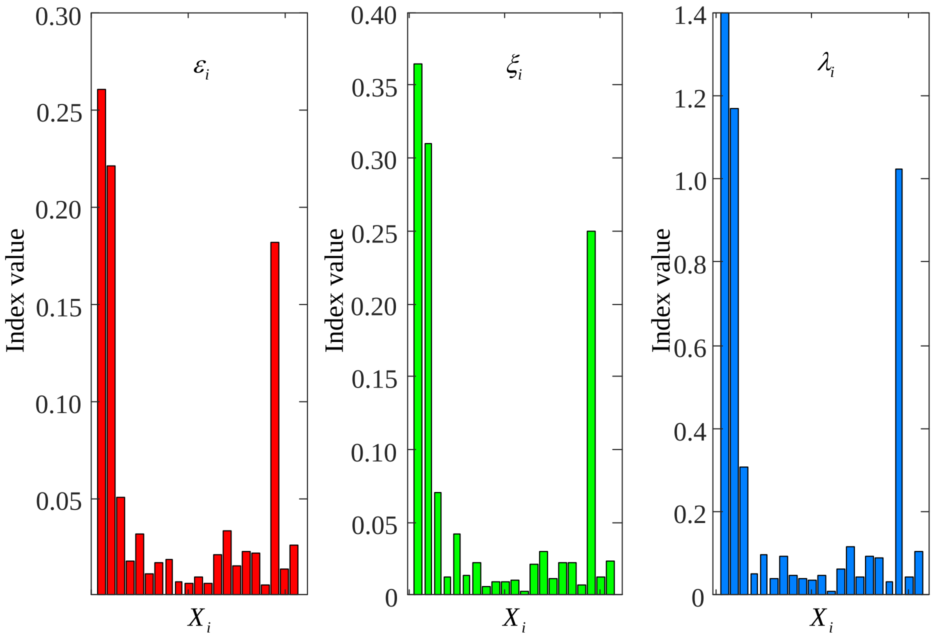

Figure 13 Results of the sensitivity indices of the radome structure in the total strain energy case

Conclusion

To address the uncertainty analysis of the non-probabilistic models, a novel sensitivity index based on non-probabilistic limit-state measure is proposed in this work. The classical non-probabilistic limit-state measure is reviewed, and the proposed sensitivity index can quantify the influence of variables on that limit-state measure. Meanwhile, the proposed sensitivity index is applicable not only for independent cases but also for dependent cases in which the interval variables contain dependences. Furthermore, an efficient computational strategy based on an adaptive Kriging surrogate model is introduced for calculation of the proposed index.

To illustrate the usefulness and validity of the proposed sensitivity index, two numerical examples involving linear and nonlinear performance functions are investigated. By comparing with the existing two sensitivity indices, the proposed index is easier to interpret and more comprehensive, and it can directly pinpoint the most influential variable on the structural limit-state measure. Moreover, the proposed sensitivity index is more inclined to quantify the changes of non-probabilistic limit-state measure from the perspective of the entire interval space and conclude different sensitivity analysis results compared with existing sensitivity indices. Finally, the proposed sensitivity index is applied to the sensitivity analysis of the composite radome to obtain the influence of variables such as different ply material performance parameters, ply angles, and ply thicknesses on the non-probabilistic limit-state measure, which are based on the structural maximum deformation and total strain energy. The identified sensitivity index ranking can provide design guidance for improving the composite radome structures from a failure state or an uncertain state towards to the safe state. In summary, the proposed sensitivity index provides an alternative for performing the sensitivity analysis of non-probabilistic models.

Data Availability Statement

Some or all data, models, or code that support the findings of this study are available from the corresponding author upon reasonable request.

Acknowledgment

This work is supported by the National Natural Science Foundation of China (Grant No. NSFC51975476).

References

Ben-Haim Y. 1993. Convex Models of Uncertainty in Radial Pulse Buckling of Shells. J Appl Mech 60:683–688. https://doi.org/10.1115/1.2900858

Ben-Haim Y. 1994. A non-probabilistic concept of reliability. Struct Saf 14:227–245. https://doi.org/https://doi.org/10.1016/0167-4730(94)90013-2

Ben-Haim Y, Elishakoff IBT-S in AM (eds). 1990. Chapter 2 - Mathematics of Convexity. In: Convex Models of Uncertainty in Applied Mechanics. Elsevier, pp 44–69

Bichon BJ, Eldred MS, Swiler LP. 2008. Efficient Global Reliability Analysis for Nonlinear Implicit Performance Functions. AIAA J 46:2459–2468. https://doi.org/10.2514/1.34321

Borgonovo E. 2007. A new uncertainty importance measure. Reliab Eng Syst Saf 92:771–784. https://doi.org/https://doi.org/10.1016/j.ress.2006.04.015

Chang Q, Zhou CC, Valdebenito MA, Liu HW, Yue ZF. 2022. A novel sensitivity index for analyzing the response of numerical models with interval inputs. Comput Methods Appl Mech Eng 400:115509. https://doi.org/10.1016/j.cma.2022.115509

Elishakoff I, Elisseeff P, Glegg SAL. 1994. Nonprobabilistic, convex-theoretic modeling of scatter in material properties. AIAA J 32:843–849. https://doi.org/10.2514/3.12062

Faes M, Moens D. 2019. Multivariate dependent interval finite element analysis via convex hull pair constructions and the Extended Transformation Method. Comput Methods Appl Mech Eng 347:85–102. https://doi.org/10.1016/j.cma.2018.12.021

Faes M, Moens D. 2020. Recent Trends in the Modeling and Quantification of Non-probabilistic Uncertainty. Arch Comput Methods Eng 27:633–671. https://doi.org/10.1007/s11831-019-09327-x

Faes MGR, Daub M, Marelli S, Patelli E, Beer, M. 2021. Engineering analysis with probability boxes: A review on computational methods. Struct Saf 93:. https://doi.org/10.1016/j.strusafe.2021.102092

Goller B, Pradlwarter HJ, Schuëller GI. 2013. Reliability assessment in structural dynamics. J Sound Vib 332:2488–2499

Guo SX, Lu ZZ. 2015. A non-probabilistic robust reliability method for analysis and design optimization of structures with uncertain-but-bounded parameters. Appl Math Model 39:1985–2002. https://doi.org/10.1016/j.apm.2014.10.026

Hanss M. 2002. The transformation method for the simulation and analysis of systems with uncertain parameters. Fuzzy Sets Syst 130:277–289. https://doi.org/10.1016/S0165-0114(02)00045-3

Helton JC. 1997. Uncertainty and sensitivity analysis in the presence of stochastic and subjective uncertainty. J Stat Comput Simul 57:3–76. https://doi.org/10.1080/00949659708811803

Jiang C, Zhang QF, Han X, Qian YH. 2014. A non-probabilistic structural reliability analysis method based on a multidimensional parallelepiped convex model. Acta Mech 225:383–395. https://doi.org/10.1007/s00707-013-0975-2

Jiang C, Zheng J, Han X. 2018. Probability-interval hybrid uncertainty analysis for structures with both aleatory and epistemic uncertainties: a review. Struct Multidiscip Optim 57:2485–2502.

https://doi.org/10.1007/s00158-017-1864-4

Kala Z. 2020. Sensitivity analysis in probabilistic structural design: A comparison of selected techniques. Sustain 12:. https://doi.org/10.3390/su12114788

Li G, Lu Z, Tian L, Xu J. 2013. The importance measure on the non-probabilistic reliability index of uncertain structures. Proc Inst Mech Eng Part O J Risk Reliab 227:651–661. https://doi.org/10.1177/1748006X13489069

Liu H, Ong YS, Cai J. 2018. A survey of adaptive sampling for global metamodeling in support of simulation-based complex engineering design. Struct Multidiscip Optim 57:393–416. https://doi.org/10.1007/s00158-017-1739-8

Lophaven SN, Nielsen HB, Sondergaard J. 2002. DACE: A Matlab Kriging Toolbox. Citeseer.

Moens D, Vandepitte D. 2007. Interval sensitivity theory and its application to frequency response envelope analysis of uncertain structures. Comput Methods Appl Mech Eng 196:2486–2496. https://doi.org/https://doi.org/10.1016/j.cma.2007.01.006

Naskar S, Mukhopadhyay T, Sriramula S. 2019. Spatially varying fuzzy multi-scale uncertainty propagation in unidirectional fibre reinforced composites. Compos Struct 209:940–967. https://doi.org/10.1016/j.compstruct.2018.09.090

Ni BY, Jiang C, Han X. 2016. An improved multidimensional parallelepiped non-probabilistic model for structural uncertainty analysis. Appl Math Model 40:4727–4745. https://doi.org/https://doi.org/10.1016/j.apm.2015.11.047

Papaioannou I, Straub D. 2021. Variance-based reliability sensitivity analysis and the FORM α-factors. Reliab Eng Syst Saf 210:107496. https://doi.org/https://doi.org/10.1016/j.ress.2021.107496

Pradlwarter HJ, Pellissetti MF, Schenk CA, Schuëller, G. I., Kreis A, Fransen S, Calvi A, Klein M. 2005. Realistic and efficient reliability estimation for aerospace structures. Comput Methods Appl Mech Eng 194:1597–1617. https://doi.org/10.1016/j.cma.2004.05.029

Regis RG, Shoemaker CA. 2007. A Stochastic Radial Basis Function Method for the Global Optimization of Expensive Functions. INFORMS J Comput 19:497–509. https://doi.org/10.1287/ijoc.1060.0182

Saltelli A. 2002. Sensitivity analysis for importance assessment. Risk Anal 22:579–590. https://doi.org/10.1111/0272-4332.00040

Simoen E, De Roeck G, Lombaert G. 2015. Dealing with uncertainty in model updating for damage assessment: A review. Mech Syst Signal Process 56–57:123–149. https://doi.org/10.1016/j.ymssp.2014.11.001

Song XM, Zhang JY, Zhan CS, Xuan YQ, Ye M, Xu CG. 2015. Global sensitivity analysis in hydrological modeling: Review of concepts, methods, theoretical framework, and applications. J Hydrol 523:739–757. https://doi.org/10.1016/j.jhydrol.2015.02.013

Wang L, Xiong C, Hu JX, Wang XJ, Qiu ZP. 2018. Sequential multidisciplinary design optimization and reliability analysis under interval uncertainty. Aerosp Sci Technol 80:508–519. https://doi.org/https://doi.org/10.1016/j.ast.2018.07.029

Wei P, Lu Z, Song J. 2015. Variable importance analysis: A comprehensive review. Reliab Eng Syst Saf 142:399–432. https://doi.org/10.1016/j.ress.2015.05.018

Zhou CC, Li C, Zhang HL, Zhao HD, Zhou CP. 2021a. Reliability and sensitivity analysis of composite structures by an adaptive Kriging based approach. Compos Struct 278:114682. https://doi.org/https://doi.org/10.1016/j.compstruct.2021.114682

Zhou CC, Zhao HD, Chang Q, Ji MY, Li C. 2021b. Reliability and global sensitivity analysis for an airplane slat mechanism considering wear degradation. Chinese J Aeronaut 34:163–170. https://doi.org/10.1016/j.cja.2020.09.048